Traversal Cost Modeling Based on Motion Characterization for Multi-legged Walking Robots

Miloš Prágr Petr Čížek Jan Faigl

***Abstract*— In this paper, we concern a traversal cost estimation considering motion control of a hexapod walking robot. The proposed idea is motivated by the observation that the traversal cost depends not only on the traversed terrain but also on the robot motion. Based on the experimental deployments, the forward motion is preferable over some terrains; however, uphill and downhill locomotion over the particular terrain might differ significantly. Therefore, we propose to enhance the traversal cost model by a motion characterization. The model is learned using feature descriptor composed of terrain shape and appearance that is combined with the expected motion performance determined from the slope change and possible rotation of the robot. The traversal model enables to reason about the robot stability regarding placement of the robot legs and performed motion action. The proposed idea of motion characterization is demonstrated and experimentally verified on a simplified motion control using grid-based planning with the robot control decomposed into straight and turn movements.**

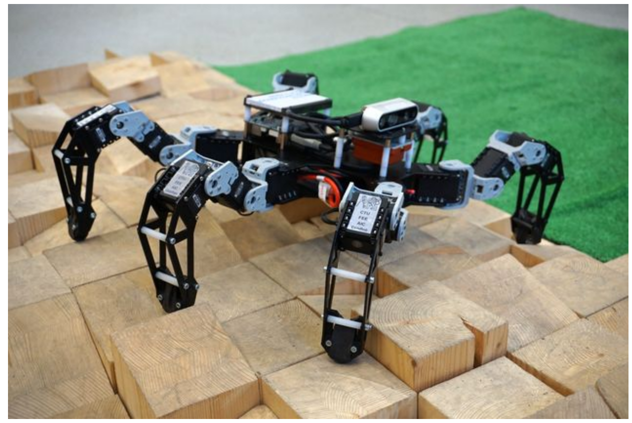

Fig. 1. The hexapod walking robot used in the experimental validation of the motion characterization proposed in this paper.

I. Introduction

This paper concerns the traversal cost modeling for multi-legged walking robots that can traverse rough terrains either by planning the exact positions of their footholds [1]–[3], or by using the feedback from their legs [4], [5]. In this work, we focus on improving the safety and performance over traversable areas, and we assume that the robot is operating in a traversable environment. Therefore, we assume that only easily recognized areas such as walls and ravines are untraversable using regular locomotion gait [6]. In our former work [7], we propose to incrementally learn the traversal cost experienced by the robot inferred from observed terrain feature descriptors. The model has been further deployed and verified in path planning scenario [8] to avoid hard to traverse areas based on the experience collected so far. In our robot deployments in various terrains, we experienced that both considered traversal costs (the energy exertion and stability of the robot attitude) depend not only on the particular terrain type but also on the direction the robot is approaching the terrain, i.e., down- and up-hill locomotion over the same terrain. Besides, we observed that forward motion is less demanding than turning movements over some terrains. Therefore, we propose to enhance the model of the traversal cost by considering motion characterization of the used robot. The proposed idea is demonstrated in the following simplified deployment of the hexapod walking robot depicted in Fig. 1 to show the need for the motion characterization in the traversal cost estimation.

It is assumed that the robot motion control is decomposed into a set of motion primitives; w.l.o.g. into 0.25 m straight forward walks and 90 degree rotations. Even though we can imagine further motion actions, the main idea of the proposed approach is to reason about the terrain and robot motion actions, for which two simple basic maneuvers are sufficient. Thus, we are concerned over what type of motion the robot executes over which terrain. We address the raised problem by enhancing the terrain descriptor by a motion descriptor that characterizes the slope of the executed motion and indicates whether the robot would change its heading. The proposed motion characterization is coupled with the terrain characterization and integrated into the robot path planner. Since we employ the incremental learning of the proposed model, the robot experience collected so far can be instantly used in path planning.

The remainder of the paper is structured as follows. In Section II, we review traversal costs and other works related to the locomotion efficiency of the multi-legged walking robots. The traversal cost model for the robot path planning is formulated in Section III. The proposed motion characterization, the related traversal cost inference method, and its application in path planning for the hexapod walking robot are presented in Section IV. Results on the experimental validation of the proposed approach are reported in Section V. Finally, the work is concluded in Section VI.

II. Review of Traversal Cost

The fundamental premise of robot motion planning is to reach the goal locations efficiently with minimized risks,

Authors are with the Czech Technical University, Faculty of Electrical Engineering, Technicka 2, 166 27, Prague, Czech Republic {milos.pragr|petr.cizek|faiglj}@fel.cvut.cz

The presented work has been supported by the Czech Science Foundation (GAČR) under research project No. 18-18858S.

energy consumption, and time. Risks incurred by mobile robots may be generalized as a chance of the system reaching a configuration without possible return. Such configurations can be caused by a wide range of threats, including the well-documented cases of the robot damage [9] and entering difficult and unsafe areas [10].

The loss of stability is related to the robot tumbling over, and thus indicates the risk of physical damage. Stability margin, also referred to as the Static Stability Margin (SSM), is a stability measure for multi-legged walking robots [11], defined as the shortest distance between the vertical projection of the robot center of gravity and either any point, vertex, or edge on the supporting polygon. The Dynamic Stability Margin (DSM) [12] replaces the vertical center of gravity projection with a projection along the direction of the combined gravitational, inertial, and external forces. The stability margin concept is further employed in the Energy Stability Margin (ESM) [13] that is defined as the minimum work required to rotate the robot center of gravity about any support polygon edge to a configuration where the center of gravity is located over that edge. Moreover, in our experience, low stability may cause the robot body vibration and thus damage of its construction, e.g., cable placement, or decreased sensor accuracy; hence it can hamper the robot localization and its perception of the environment. Besides, vehicle vibration may cause harm to passengers [14], but vibration can be utilized as a terrain type descriptor. For example a vibration based classifier has been used to identify terrains encountered by passenger vehicles [15] and to characterize simulated Martian terrains [16].

Low traversal efficiency can also be considered as a risk factor, since a robot may enter a configuration from which it is impossible to move out, e.g., wasting its battery while not reaching its goal or reaching a location inside a hole in the ground. The cost of transport [17] is a measure of the energy efficiency of motion, defined as the ratio of the consumed power and reached velocity over a particular terrain type. The authors of [18] employ the concept of the cost of transport to the battery-powered vehicle, where the power consumption is based on the instantaneous current drawn from the robot battery, and the measure is normalized by the robot mass and gravitation acceleration to get a dimensionless quantity.

Exteroceptive approaches are utilized to extrapolate possible traversal risks of observed but not yet visited areas. A traversal cost is assigned to the observed area, e.g., a cost that defines a danger, complication, or roughness of the terrain. The exteroceptive properties of the observed terrain can be utilized to 1) directly compute properties closely related to the terrain traversability, e.g., geometric properties such as roughness; 2) assign terrain classification from the labeled data; or 3) both approaches can be combined. Classification methods divide observed terrain into a set of predetermined classes that can be human defined terrain types [16], but it can also be identified as an untraversable obstacle class [20].

Direct exteroceptive traversal efficiency characterization suffers from limited adaptability, as it is based on predetermined geometrical or classification setups. However, exteroceptive approaches may be utilized as terrain descriptors in more complex traversability estimation schemata.

The existing geometric descriptors related to the terrain traversability are based on the height and slope [20]–[24]. The height and slope based measures need to be referenced to the ground coordinate frame, which can be an issue when encountering generally sloped environments such as mountainsides. Height based measures utilize mean and deviation statistics [20], [21] or observed the necessary step height [21]–[23]. Slope measures range from the gradient based [24], through local-vs-global plane [21], [22] to normal based [20], [23]. Alternatively, the terrain roughness can be characterized by eigen-statistics of the local neighborhood of the particular location of interest. In [20], [25], the authors use a set of eigenvalue features designed to discriminate flat, vegetated, and obstructed terrains.

A combination of the height variance roughness, height difference, step height, and circular neighborhood slope to the ground is utilized for the terrain evaluation in [21]. A set of seven features to characterize the step height and roughness is used in [22].

In addition to the terrain characterization using a set of descriptors, the autonomous robots operating in potentially dangerous areas must predict traversal efficiency of their planned motion. Although it does not imply that an efficiency model is learned, it is often the case for traversal efficiency not defined as a direct consequence of the observed data, e.g., directly from geometric properties of the terrain as in [21]. The authors of [26] combine SVM classifier on robot vibration with Gaussian mixture clustering on visual data to classify terrain into five classes: grass, asphalt, gravel, pavement, and indoor flooring. On the other hand, two SVMs are utilized in co- and self-training setup by the authors of [16]. An online Bayesian framework is utilized in [27] for modeling the global and locale-specific terrain descriptors.

In [7], we propose to learn the cost of transport [18] incrementally from a terrain feature descriptor, and thus combining the advantages of robot-observed proprioceptive locomotion efficiency with the exteroceptive terrain characterization. In this paper, we leverage the work [7], and we extend the feature descriptor to include the proposed motion characterization. Moreover, we choose to represent the traversal cost based on the observed robot stability to characterize risks encountered with the hexapod walking robot, which better fits to risk assessment than usage of the cost of transport. However, we avoid the foothold position calculation by using a measure based on robot attitude instead of a stability margin approach.

III. Problem Formulation

The proposed enhancement of the traversal cost model by motion characterization is motivated by the deployment of a multi-legged walking robot in rough terrains, where it is desirable to discriminate paths according to the safety and efficiency of the robot motion. The paths need to be selected with regards to the traversal cost prediction for the observed terrain. The robot motion control is decoupled into two actions: $0.25\,\mathrm{m}$ long *forward* walks, which correspond roughly to the distance covered by two gait cycles, and *turn* about 90 degrees. Even though the robot has eighteen controllable joints, based on the motion actions, simplified state of the robot is considered as $\boldsymbol{q} = (x, y, \phi)$ and it consists of the location (x, y) considered within a grid-based environment representations with the squared cell size $0.25\,\mathrm{m}$, and the discretized heading $\phi \in \{0, \frac{\pi}{2}, \pi, \frac{3\pi}{2}\}$. The motion planning problem is defined as a problem to find a sequence of actions (forward walks or turns) to move the robot from one grid cell to the desired destination cell. For simplicity and focused presentation of the proposed idea of motion characterization, we assume the robot is operating only in a traversable environment; however, we further distinguish the motion safety that is directly related to the configuration of the robot legs and the used footholds. Therefore, the robot planned motion is limited to such configurations.

The assessment of the robot safety at the robot state $\boldsymbol{q}$ is based on the position of the robot footholds [2]. However, a simplification based on a mask of possible leg positions is utilized to characterize the embodiment of the robot. The mask is oriented according to the robot heading shown in Fig. 2a. The mask represents the ground projection of the six footholds that are further accompanied by the robot center of gravity. The safety of the state is related to the position and the relative elevation of the footholds, and therefore, we investigate the slope between the selected pairs of the robot footholds. The slope $\alpha(X^{\boldsymbol{q}}, Y^{\boldsymbol{q}'})$ between the legs X and Y for states $\boldsymbol{q}$ and $\boldsymbol{q}'$, respectively, is schematically visualized in Fig. 2b and Fig. 2c. The slope can be defined as

$$\alpha(X^{\boldsymbol{q}}, Y^{\boldsymbol{q}'}) = \arctan\frac{\|z_{\mathrm{X}}^{\boldsymbol{q}} - z_{\mathrm{Y}}^{\boldsymbol{q}'}\|}{\|(x_{\mathrm{X}}^{\boldsymbol{q}}, y_{\mathrm{X}}^{\boldsymbol{q}}) - (x_{\mathrm{Y}}^{\boldsymbol{q}'}, y_{\mathrm{Y}}^{\boldsymbol{q}'})\|}, \qquad (1)$$

where z is the elevation of the environment. For the particular hexapod robot used in the experimental verification, the state $\boldsymbol{q}$ is considered safe if the following holds

$$\begin{aligned}
&|\alpha(LR^{\boldsymbol{q}}, RR^{\boldsymbol{q}})| < \frac{\pi}{4} \wedge |\alpha(LC^{\boldsymbol{q}}, CoG^{\boldsymbol{q}})| < \frac{\pi}{4} \wedge \\
&\wedge|\alpha(CoG^{\boldsymbol{q}}, RC^{\boldsymbol{q}})| < \frac{\pi}{4} \wedge |\alpha(LF^{\boldsymbol{q}}, RF^{\boldsymbol{q}})| < \frac{\pi}{4} \wedge \\
&\wedge|\alpha(LF^{\boldsymbol{q}}, LC^{\boldsymbol{q}})| < \frac{\pi}{4} \wedge |\alpha(LC^{\boldsymbol{q}}, LR^{\boldsymbol{q}})| < \frac{\pi}{4} \wedge \\
&\wedge|\alpha(RF^{\boldsymbol{q}}, RC^{\boldsymbol{q}})| < \frac{\pi}{4} \wedge |\alpha(RC^{\boldsymbol{q}}, RR^{\boldsymbol{q}})| < \frac{\pi}{4},
\end{aligned} \qquad (2)$$

where $\wedge$ denotes the logical and operator, and symbols for the footholds and center of gravity (CoG) are as in Fig. 2.

Similarly, a motion from the state $\boldsymbol{q}$ to the state $\boldsymbol{q}'$ is considered safe if both states are safe and the motion $(\boldsymbol{q}, \boldsymbol{q}')$ is safe as well. The safety is determined from foothold positions and the projected CoG as the slope between the foothold positions $\boldsymbol{q}$ and $\boldsymbol{q}'$ and the motion $(\boldsymbol{q}, \boldsymbol{q}')$ is assumed to be safe if (3) holds.

$$\begin{aligned}
&|\alpha(LR^{\boldsymbol{q}}, LR^{\boldsymbol{q}'})| < \frac{\pi}{4} \wedge |\alpha(LC^{\boldsymbol{q}}, LC^{\boldsymbol{q}'})| < \frac{\pi}{4} \wedge \\
&\wedge|\alpha(LF^{\boldsymbol{q}}, LF^{\boldsymbol{q}'})| < \frac{\pi}{4} \wedge |\alpha(RR^{\boldsymbol{q}}, RR^{\boldsymbol{q}'})| < \frac{\pi}{4} \wedge \\
&\wedge|\alpha(RC^{\boldsymbol{q}}, RC^{\boldsymbol{q}'})| < \frac{\pi}{4} \wedge |\alpha(RF^{\boldsymbol{q}}, RF^{\boldsymbol{q}'})| < \frac{\pi}{4} \wedge \\
&\wedge|\alpha(CoG^{\boldsymbol{q}}, CoG^{\boldsymbol{q}'})| < \frac{\pi}{4} \wedge \boldsymbol{q} \text{ and } \boldsymbol{q}' \text{ are safe}
\end{aligned} \qquad (3)$$

Finally, the traversal cost c is measured as the root of the variance of the robot roll observed over the $10\,\mathrm{s}$ period, which corresponds to the average expected time for traversing a single grid cell. The learned traversal cost model is used to infer the cost $\hat{c}$ using the motion feature characterization. The cost $c(\boldsymbol{q}, \boldsymbol{q}')$ corresponding to the motion between the states $\boldsymbol{q}$ and $\boldsymbol{q}'$ is defined as

$$c(\boldsymbol{q}, \boldsymbol{q}') = \|\boldsymbol{q}, \boldsymbol{q}'\| + \lambda_{\mathrm{cost}}\hat{c}(\boldsymbol{q}, \boldsymbol{q}'), \qquad (4)$$

where $\|\boldsymbol{q}, \boldsymbol{q}'\|$ is the Euclidean distance between the coordinates corresponding to the state $\boldsymbol{q}$ and $\boldsymbol{q}'$, the prediction of the traversal cost is $\hat{c}(\boldsymbol{q}, \boldsymbol{q}')$, and $\lambda_{\mathrm{cost}} = 100$ is the cost-to-distance scaling constant. Thus, the cost of a motion sequence is the robot walking distance summed with the traversal cost prediction for each of the motion actions. Since we assume two types of motion actions and a grid with the squared cell size $0.25\,\mathrm{m}$, two instances of (4) are as follows.

1) The cost to execute the 0.25 m forward motion can be defined as

$$c_{\mathrm{forward}}(\boldsymbol{q}, \boldsymbol{q}') = 0.25 + 100\hat{c}(\boldsymbol{q}, \boldsymbol{q}'), \qquad (5)$$

2) and the cost to turn by 90 degrees as

$$c_{\mathrm{turn}}(\boldsymbol{q}, \boldsymbol{q}') = 100\hat{c}(\boldsymbol{q}, \boldsymbol{q}'). \qquad (6)$$

IV. Path Planning with Motion Characterization

The motion of the utilized hexapod walking robot is characterized by the feature descriptor of the traversed terrain combined with the motion characterization. The observed descriptors are used to learn the traversal cost model that is used for the prediction of the traversal cost in path planning according to (4), and the robot path, i.e., the cheapest sequence of motion actions, is selected using the A* with the Euclidean distance heuristic. In particular, we deploy feature descriptors of the terrain shape and appearance and characterize the motion by slope and rotation. Thus, the feature descriptor is the seven-dimensional vector $\boldsymbol{d} = (s_1, s_2, s_3, a_1, a_2, m_1, m_2)$, where shape and appearance features, which are based on the previous work [7], are denoted $(s_1, s_2, s_3, a_1, a_2)$ and characterize the traversed terrain in the 0.2 m radius neighborhood around the investigated location of the robot. The shape descriptors are based on eigenvalues statistics extracted for the defined neighborhood area [20], and the appearance part describes the neighborhood terrain color in the Lab color space.

The design of the descriptor characterizing the motion stems from the made observations that the energy exertion and stability experience is different for the same area but

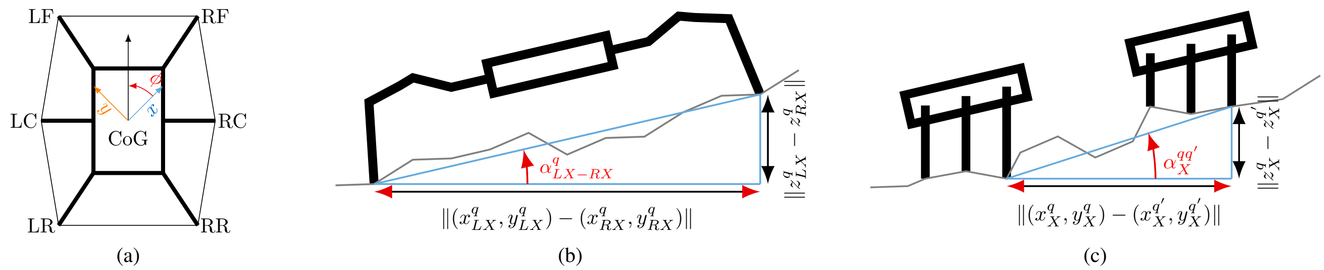

Fig. 2. The proposed (a) simplified foothold mask applied to the robot state $\boldsymbol{q} = (x, y, \phi)$, (b) slope between the left and right legs LX and RX for the state $\boldsymbol{q}$, and (c) forward motion slope between the foothold positions of the leg X for the states $\boldsymbol{q}$ and $\boldsymbol{q}'$.

down- and up-hill locomotion. Similarly, the forward motion is less demanding than turning over some terrains. Hence, the motion characterization is proposed as the descriptors (m_1, m_2). The forward motion action is proposed to be characterized as the slope feature

$$m_1 = \arctan \frac{\|\Delta z\|}{\|\Delta(x, y)\|}, \tag{7}$$

where $\|\Delta z\|$ is the elevation change, and $\|\Delta(x, y)\|$ is the Euclidean distance on the ground plane covered by the described motion. The rotation motion is proposed to be characterized by the feature m_2 defined as

$$m_2 = \arctan \frac{\|\Delta \phi\|}{\|\Delta(x, y, z)\|}, \tag{8}$$

where $\|\Delta\phi\| \in (0, \pi)$ is the absolute value of the robot heading change, and $\|\Delta(x, y, z)\|$ is the Euclidean distance traversed by the robot. Notice that $\arctan$ function is utilized to scale the feature to $(0, \frac{\pi}{2})$ and has no geometric interpretation, unlike in (7).

Before a detailed description of the traversal cost model learning process, we first remind the reader that the traversal cost c is measured as the root of the variance of the robot roll observed over the $10\,\mathrm{s}$ long period. The descriptor $\boldsymbol{d}$ is paired with the experienced cost c in the robot experience descriptor $\boldsymbol{d}_c = (s_1, s_2, s_3, a_1, a_2, m_1, m_2, c)$. The descriptor $\boldsymbol{d}_c$ thus characterizes the robot motion executed over the $10\,\mathrm{s}$ long period. Notice that both the motion action and the period used to measure the traversal cost are roughly equal to two gait cycles of the employed locomotion controller of the utilized hexapod walking robot.

The traversal cost model is learned using the Incremental Gaussian Mixture Network (IGMN) [28], which incrementally builds a Gaussian mixture model from a single scan of data, and thus can be used in life-long learning scenarios. The IGMN is parameterized with the $k = 10$ components, grace period $v_{\text{min}} = 100$, minimal accumulated posterior $sp_{\text{min}} = 3$, and scaling factor $\delta = 1$. The model $M(k)$, which incorporates k observations, is a result of the incremental update

$$M(k) \leftarrow \mathit{update}(M(k-1), \boldsymbol{d}_c). \tag{9}$$

The traversal cost prediction $\hat{c}$ is obtained by querying the traversal cost model M for the descriptor $\boldsymbol{d}$. The descriptor $\boldsymbol{d}$ is used for cost prediction of the motion action, and thus particular values of m_1 and m_2 in $\boldsymbol{d}$ are considered. The shape and appearance part of $\boldsymbol{d}$ characterizes the terrain corresponding to the area of the states $\boldsymbol{q}$ and $\boldsymbol{q}'$ that define the start and end of the motion, respectively. Thus, the shape and appearance descriptors are computed for the neighborhood centered at the geometric center of the straight line segment connecting the states $\boldsymbol{q}$ and $\boldsymbol{q}'$.

V. Experimental Verification

The proposed approach has been verified in two experimental scenarios from which the achieved results are reported in this section. First, the influence of the executed motion on the traversal cost experienced by the robot is demonstrated to support the motivation of the addressed problem experimentally. Second, the robot was deployed on the laboratory test track to demonstrate the incremental learning of the traversal cost model and its applicability in path planning. The robot showed in Fig. 1 has been utilized in both scenarios, and its detailed specification can be summarized as follows.

The robot is about $50 \times 60 \times 20$ cm large. Each of its six legs consists of three joints actuated by the Dynamixel AX-12A servo motors. For locomotion with the forward velocity up to $0.05\,\mathrm{ms}^{-1}$, the robot employs the tripod adaptive motion gait [4], which is decomposed into the leg swing phase and the body leveling phase. The robot is navigated along the planned path using the follow-the-carrot algorithm with $0.2\,\mathrm{m}$ threshold distance. ORB-SLAM2 [29] with the Intel RealSense D435 RGB-D camera with the resolution 640×480 px and $30\,\mathrm{Hz}$ are utilized for the robot localization. The XSense MTi-30 attitude heading reference system is used to capture the robot roll at $400\,\mathrm{Hz}$. The proposed approach has been implemented in ROS [30] and computational requirements of the individual parts of the complete navigation pipeline are reported in Table I.

TABLE I

Performance of the Proposed System on the Intel i7 8550U

Process	CPU usage*	Update frequency
Localization - ORB-SLAM2 [29]	130%	14.00 Hz
Traversal cost calculation	31%	400.00 Hz
Feature extraction and model learning	327%	0.50 Hz
Planning and cost inference	105%	0.05 Hz
Locomotion control	70%	62.50 Hz

*The reported usage is of 800% because 4 × cores with Hyper-threading

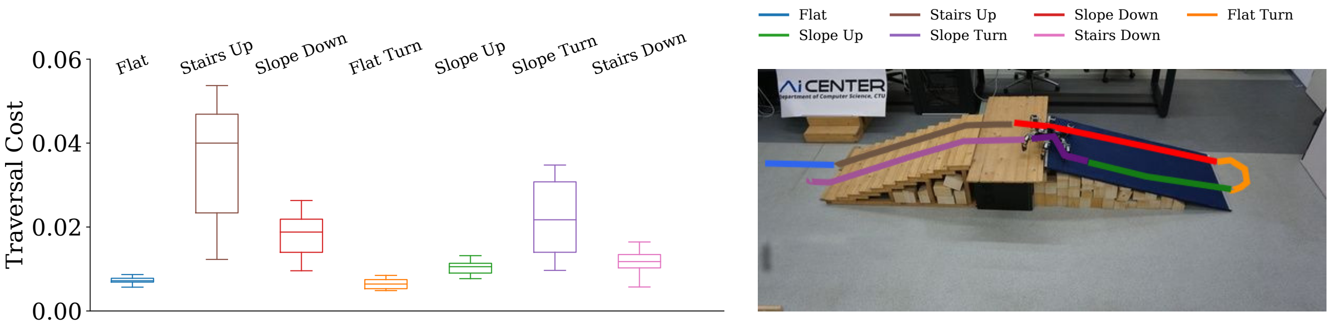

Fig. 3. The traversal costs observed by the hexapod walking robot (left) while traversing over a raised obstacle (right).

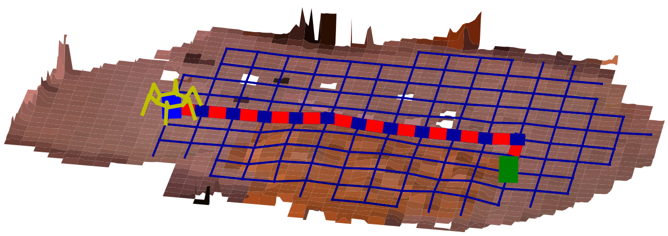

(a) Traversal cost assessment before the experiment.

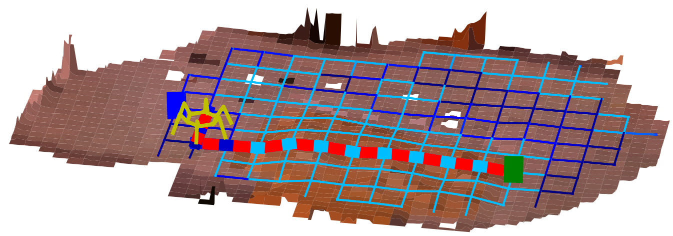

(b) Cost assessment after walking over the flat ground.

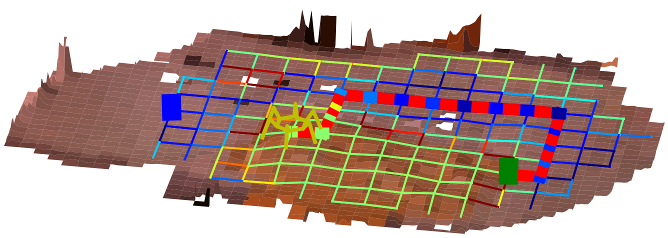

(c) Cost assessment after walking over the wooden blocks.

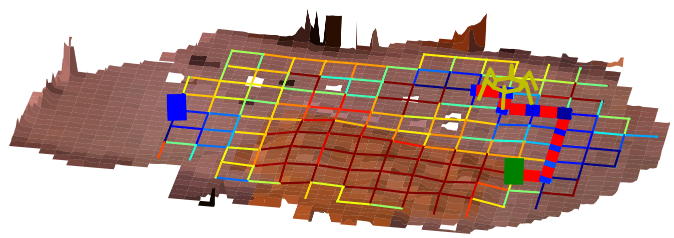

(d) Cost assessment after leaving the blocks.

Fig. 4. Snapshots of the traversal cost assessments during autonomous navigation with incremental traversal cost learning. Straight lines represent predicted motion cost using forward walk motion action. The dashed red lines represent the determined cheapest motion sequence towards the goal location, which is shown as a green rectangle. The test track consists of flat ground and wooden blocks of uneven height, and it is shown in Fig. 5. The wooden blocks are hard to traverse because of their relative size to the robot, but the flat ground around the blocks is easy to traverse. From the initial location, based on the learned traversal cost model, the robot may either reach the goal location over the rough terrain or choose a longer flat route, which is however cheaper regarding (4). After traversing the border of the wooden blocks, the robot avoids further traversal of the rough terrain and chooses the longer route.

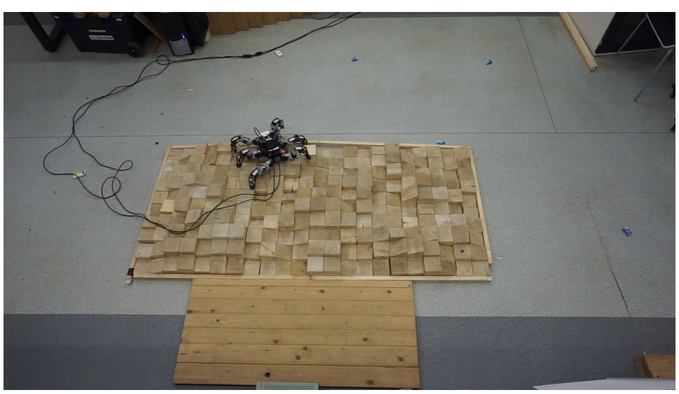

Fig. 5. The laboratory test track used for the experimental deployment.

A. *Influence of Executed Motion*

The robot is guided over a raised obstacle, see Fig. 3b, to demonstrate the influence of the executed motion on the traversal cost experienced by the robot. The costs experienced traversing the individual parts of the path are shown in Fig. 3a. The robot firstly walks over the flat ground, ascends the wooden stairs and descends a flat, but sloped surface. After that, the robot turns on the flat ground, and walks back over the obstacle. Based on the reported experimental results, we can make observations that reinforce the importance of the particular motion action to the experienced traversal cost. Although it is costly to ascend the stairs, it is much cheaper to descend, possibly because the adaptive motion gait gets stuck on the individual steps when ascending. However, it is cheaper to ascend the sloped surface than to descend or turn on it. This might be explained by the robot slipping while trying to descend to sloped terrain. We can conclude that there are considerable differences in the costs to ascend and descend over different terrains and also turning might be costly in comparison to ascending. Therefore, it is desirable to include the robot motion into the reasoning about the traversal cost.

B. *Incremental Learning of the Traversal Cost Model*

The indoor track shown in Fig. 5 has been used for the experimental deployment of the proposed approach with the incremental model learning, path planning, and autonomous navigation. The track consists of wooden blocks with irregular height accompanied by the easy to traverse flat ground.

The evolution of the traversal cost and determined robot path towards the goal are shown in Fig. 4. After the robot encounters the wooden blocks, it learns the cost over the wooden blocks is high, see Fig. 4c. Specifically, climbing up or down over the boundary of the wooden blocks is costly. Thus, the robot climbs down the wooden blocks and walks towards its goal over the flat ground. When leaving the blocks, the robot encounters the hard to traverse the edge of the rough terrain that further increases the cost of the wooden blocks. Moreover, the robot suffers from instability for a few seconds, affecting the cost of the flat ground; however, the cheapest path is determined over the flat ground, see Fig. 4d.

The presented experimental results support the proposed approach, and the robot incrementally learns the traversal cost of its motion over individual terrains, and it applies the gained knowledge in reasoning about the cost-efficient path.

VI. Conclusion

In this paper, we propose to enhance the existing incremental learning of the traversal cost by characterization of the robot motion over the traversed terrains. The proposed concept of the motion characterization is demonstrated in grid-based planning considering two motion actions of the hexapod walking robot. The terrain shape and appearance features are enhanced by the robot motion characterized as feature descriptors of the expected slope of the motion and rotation. The reported experimental results support that the proposed approach is feasible and demonstrate the robot motion over various terrains influences the traversal cost. The deployment of the proposed motion characterization in path planning enables the robot to learn and then avoid hard to traverse areas in autonomous navigation missions. In our future work, we aim to generalize the proposed concept to other motion actions using motion planning techniques, such as randomized sampling-based algorithms.

References

[1] M. Hutter, C. Gehring, D. Jud, A. Lauber, C. D. Bellicoso, V. Tsounis, J. Hwangbo, K. Bodie, P. Fankhauser, M. Bloesch, R. Diethelm, S. Bachmann, A. Melzer, and M. Hoepflinger, "ANYmal - a highly mobile and dynamic quadrupedal robot," in *IEEE/RSJ Int. Conf. Intelligent Robots and Systems (IROS)*, 2016, pp. 38–44.

[2] P. Čížek, D. Masri, and J. Faigl, "Foothold Placement Planning with a Hexapod Crawling Robot," in *IEEE/RSJ Int. Conf. Intelligent Robots and Systems (IROS)*, 2017, pp. 4096–4101.

[3] S. Bartoszyk, P. Kasprzak, and D. Belter, "Terrain-aware motion planning for a walking robot," in *International Workshop on Robot Motion and Control (RoMoCo)*, 2017, pp. 29–34.

[4] J. Faigl and P. Čížek, "Adaptive locomotion control of hexapod walking robot for traversing rough terrains with position feedback only," *Robotics and Autonomous Systems*, vol. 116, pp. 136–147, 2019.

[5] G. Bledt, M. J. Powell, B. Katz, J. D. Carlo, P. M. Wensing, and S. Kim, "MIT Cheetah 3: Design and Control of a Robust, Dynamic Quadruped Robot," in *IEEE/RSJ Int. Conf. Intelligent Robots and Systems (IROS)*, 2018, pp. 2245–2252.

[6] G. Dudek and M. Jenkin, *Computational Principles of Mobile Robotics*. New York, NY, USA: Cambridge University Press, 2000.

[7] M. Prágr, P. Čížek, and J. Faigl, "Cost of Transport Estimation for Legged Robot Based on Terrain Features Inference from Aerial Scan," in *IEEE/RSJ Int. Conf. Intelligent Robots and Systems (IROS)*, 2018, pp. 1745–1750.

[8] ——, "Incremental learning of traversability cost for aerial reconnaissance support to ground units," in *Modelling and Simulation for Autonomous Systems (MESAS)*, 2019, pp. 412–421.

[9] F. Keating, "The 'suicidal robot' that drowned in a fountain didn't kill itself after all," *Independent*, 2017.

[10] D. Brown and G. Webster, "Now a stationary research platform, nasa's mars rover spirit starts a new chapter in red planet scientific studies," *NASA Press Release*, 2010.

[11] R. B. McGhee and A. A. Frank, "On the stability properties of quadruped creeping gaits," *Mathematical Biosciences*, vol. 3, pp. 331–351, 1968.

[12] B. Lin and S. Song, "Dynamic modeling, stability and energy efficiency of a quadrupedal walking machine," in *IEEE Int. Conf. Robotics and Automation (ICRA)*, 1993, pp. 657–670.

[13] D. Messuri and C. Klein, "Automatic body regulation for maintaining stability of a legged vehicle during rough-terrain locomotion," *Robotics and Automation*, vol. 1, no. 3, pp. 132–141, 1985.

[14] S. Milosavljevic, F. Bergman, B. Rehn, and A. B. Carman, "All-terrain vehicle use in agriculture: Exposure to whole body vibration and mechanical shock," *Applied Ergonomics*, vol. 41, no. 4, pp. 530–535, 2010.

[15] C. C. Ward and K. Iagnemma, "Speed-independent vibration-based terrain classification for passenger vehicles," *Vehicle System Dynamics*, vol. 47, no. 9, pp. 1095–1113, 2009.

[16] K. Otsu, M. Ono, T. J. Fuchs, I. Baldwin, and T. Kubota, "Autonomous Terrain Classification with Co- and Self-Training Approach," *Robotics and Automation Letters*, vol. 1, no. 2, pp. 1–6, 2016.

[17] V. A. Tucker, "The Energetic Cost of Moving About: walking and running are extremely inefficient forms of locomotion. Much greater efficiency is achieved by birds, fish and bicyclists," *American Scientist*, vol. 63, no. 4, pp. 413–419, 1975.

[18] N. Kottege, C. Parkinson, P. Moghadam, A. Elfes, and S. P. N. Singh, "Energetics-informed hexapod gait transitions across terrains," in *IEEE Int. Conf. Robotics and Automation (ICRA)*, 2015, pp. 5140–5147.

[19] D. M. Bradley, J. K. Chang, D. Silver, M. Powers, H. Herman, P. Rander, and A. Stentz, "Scene Understanding for a High-mobility Walking Robot," in *IEEE/RSJ Int. Conf. Intelligent Robots and Systems (IROS)*, 2015, pp. 1144–1151.

[20] M. Kragh, R. N. Jørgensen, and H. Pedersen, "Object Detection and Terrain Classification in Agricultural Fields Using 3d Lidar Data," in *International Conference on Computer Vision Systems*, vol. 9163, 2015, pp. 188–197.

[21] A. Stelzer, H. Hirschmüller, and M. Görner, "Stereo-vision-based navigation of a six-legged walking robot in unknown rough terrain," *International Journal of Robotics Research*, vol. 31, no. 4, pp. 381–402, 2012.

[22] T. Homberger, M. Bjelonic, N. Kottege, and P. V. K. Borges, "Terrain-dependant Control of Hexapod Robots using Vision," in *International Symposium on Experimental Robotics (ISER)*, 2016, pp. 92–102.

[23] J. Gu, Q. Cao, and Y. Huang, "Rapid traversability assesment in 2.5 d grid based map on rough terrain," *International Journal of Advanced Robotics*, vol. 5, no. 4, 2008.

[24] M. Brunner, B. Brüggemann, and D. Schulz, "Rough Terrain Motion Planning for Actuated, Tracked Robots," in *International Conference on Agents and Artificial Intelligence (ICAART)*, 2013, pp. 40–61.

[25] N. Vandapel, D. Huber, A. Kapuria, and M. Hebert, "Natural terrain classification using 3-d ladar data," in *IEEE Int. Conf. Robotics and Automation (ICRA)*, New Orleans, LA, USA, 2004, pp. 5117–5122.

[26] W. Mou and A. Kleiner, "Online Learning Terrain Classification for Adaptive Velocity Control," in *IEEE Safety Security and Rescue Robotics (SSSR)*, 2010, pp. 1–7.

[27] S. Boris, E. Lin, J. A. Bagnell, J. Cole, N. Vandapel, and A. Stentz, "Improving Robot Navigation Through Self-Supervised Online Learning," *Journal of Field Robotics*, vol. 23, no. 11-12, pp. 1059–1075, 2006.

[28] R. Pinto, P. Engel, and P. Alegre, "A Fast Incremental Gaussian Mixture Model," *PLOS*, p. e0141942, 2015.

[29] R. Mur-Artal and J. D. Tardos, "ORB-SLAM2: an Open-Source SLAM System for Monocular, Stereo and RGB-D Cameras," *Transactions on Robotics*, vol. 33, no. 5, pp. 1255–1262, 2017.

[30] M. Quigley, K. Conley, B. P. Gerkey, J. Faust, T. Foote, J. Leibs, R. Wheeler, and A. Y. Ng, "ROS: an open-source robot operating system," in *ICRA Workshop on Open Source Software*, 2009.